Microsystem Technologies 9 (2003) 480–483 © Springer-Verlag 2003
DOI 10.1007/s00542-002-0278-3

Micromachining of highly reproducible step substrates for high *Tc* step junction dc-SQUIDs

J. Wang, B. Han, G. Chen, Q. Yang, T. Cui

Abstract A means to successfully fabricate highly reproducible $SrTiO_3$ step substrates for high T_C dc-Superconducting Quantum Interference Devices (dc-SQUIDs) by micromachining is reported in this paper. At optimized Ar ion milling conditions, an inclined angle from 45 to 50° and a laid angle from 30 to 45°, the highest step angles can be obtained. Under strict process control, the profile of the Nb mask film is clean and sharp. The fabricated step angles are about 71° with steep and flawless topography. The step substrate yield for $YBa_2Cu_3O_{7-x}$ Josephson step edge junction dc-SQUIDs is 75%. The variation of junction resistance and critical current is ±28.6% and ±42.4% respectively.

1
Introduction

The interdisciplinary use of lithographic, micromachining and other microfabrication technologies to prepare miniaturized, reliable, and inexpensive sensors, actuators, and circuit components has made tremendous breakthroughs in numerous modern fields such as mechanical [1], optical [2], thermal [3], chemical [4], biological [5], fluidic [6], and magnetic [7] technologies. Among all the magnetic sensors, Superconducting Quantum Interference Devices (SQUIDs) are the most sensitive magnetometers and they are the only viable sensors for detecting the magnetic fields weaker than the order of 10^{-9} T [8].

Since the advent of the high temperature critical transition (high T_C) superconductor [9], the research on interference devices based on the Josephson junction has been developed quickly [10, 11]. In order to obtain better resolution performance, the Josephson junctions have evolved from the natural grain junction to the bi-crystal junction [12], bi-epitaxial junction [13], step edge junction [14, 15], and other fabricated controllable grain junctions [16]. Compared with other junctions, the step edge junction has such advantages as structure simplicity, low cost, and little topographic limitation. However, the process control for the step substrate is tricky and the ratio of superconducting film thickness to step height is strict, which makes the yield of step edge junction relatively low. In this paper, a micromachining technique is described for better process control so that a highly reproducible means to fabricate a step substrate for dc-SQUIDs is derived.

Different from rf-SQUID, which only has one junction, dc-SQUID is comprised of two junctions. Moreover, these two junctions must be exactly the same. In order to avoid film unevenness caused by plasma direction during film deposition, junctions should be placed at the same wall of one step. In addition, they must be patterned as close as possible so that the junction parameters are almost identical. Because of the above requirements, the step bank line needs to be long enough to accommodate two junctions and consistent enough to keep these two junctions the same.

The step angle should also meet some criteria in order to ensure the 90° grain boundary [17–19]. If step angle is larger than 45° but less than 60°, (1 0 3) (1 0 3) grain boundaries are formed at both the upper and lower step edges and these two junctions are in series when $YBa_2Cu_3O_{7-x}$ (YBCO) film is epitaxially grown on the substrate. If the step angle is larger than 60°, the grain boundaries are no long symmetric. The upper is the (1 0 3) (1 0 3) boundary while the lower is the (0 0 1) (0 1 0) boundary [20]. Because the lower (0 0 1) (0 1 0) boundary is much weaker than the upper one, the total junction behaves like only one lower boundary [21]. In order to seek lower device noise, a higher step angle is necessary due to its single boundary characteristics.

The challenging work here is to fabricate high step angle, flawless topography substrates with a high product yield by micromachining.

2
Experiments

2.1
Choice of substrate

The most commonly used single crystal substrates for YBCO superconducting films are $LaAlO_3$ and $SrTiO_3$ (STO). The former has better high frequency response while the latter has better crystal match. Here only STO substrate is discussed because dc-SQUIDs only operate at low frequency.

2.2
Choice of metal mask

There are two considerations when choosing a metal mask for substrate ion milling. One consideration is that the

Received: 5 April 2002/Accepted: 9 August 2002

J. Wang, B. Han, G. Chen, Q. Yang
Institute of Physics and Center for Condensed Matter Physics, Chinese Academy of Sciences, Beijing 100080, China

J. Wang (✉), T. Cui
Institute for Micromanufacturing,
Louisiana Tech University, Ruston, LA 71272, USA
E-mail: jwa009@beta.latech.edu

metal should be as hard as possible. The other consideration is that the metal should be easily removable from the substrate so as not to influence the growth of YBCO superconducting film. Here Nb is selected as the metal mask material for convenience though other choices are also reasonable [22].

2.3 Fabrication process

Before processing, the substrates need to be well cleaned with DI water, acetone, and IPA until there is no submicron dust visible on the surface under microscopy. The substrates are then put into a chamber for metal mask sputtering. The base pressure is less than 5×10^{-3} Pa, the Ar pressure is 3 Pa and the sputtering rate is 800 Å/min with a total Nb film thickness of 4000 Å. The mask film is then patterned by photolithography. The developing time should be well controlled so that no residue is left at the bed area to affect the following process and no saw-toothed profiles arise due to over development. The following reactive etching by CF_4 gas includes two steps: removing photo resist residue and etching the Nb film. The first step lasts about 30–60 s while the second step 100–200 s. In order to get a steep Nb profile, time control is necessary, which is illustrated later.

After soaking in acetone to remove photo resist, the substrates are laid into a chamber at some orientation. At a certain Ar^+ ion milling incidence angle, the steps are etched with a height of 2500 Å. Later, the Nb film is under a CF_4 gas ambient, where another reactive etching is performed. With a thorough Nb film removal, substrates with a high step angle are fabricated. All the processes above are shown in Fig. 1.

YBCO superconducting films are deposited on prepared step substrates by pulsed laser deposition (PLD) with a thickness of about 2000 Å, which is about 70–80% of the step height. The two shunted junctions located at the same wall of the steps are patterned by photolithography and dry etching. At last, dc-SQUIDs are measured in a magnet shield system, whose environment magnetic field is less than 0.5 nT.

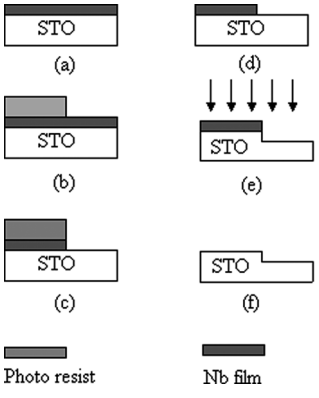

Fig. 1a–f. Step substrate fabrication process. **a** Nb mask film sputtering, **b** photolithography mask, **c** reactive etching Nb film, **d** resolve photo resist, **e** Ar^+ ion milling and **f** remove Nb

3 Results and discussion

3.1 Optimum conditions for ion milling

As discussed above, a higher step angle will cause pure junction behavior, which always means noise of dc-SQUIDs. However, 90° step angles are very hard to obtain due to secondary deposition effects at local area milling. During the ion milling, the back sputtering material at local area causes re-deposition on the step wall. Both the etching and depositing processes exist and determine the step angle θ. When these two effects are at dynamic balance, the step angle is formed. It is reasonable to assume that fast substrate etching and slow mask etching will produce a higher step angle.

In order to strictly control the milling conditions, the relations of milling rate, obtained step angle, and substrate orientation are investigated in detail. The concept of an inclined angle and a laid angle of an ion beam is shown in Fig. 2. The angle between the horizontal plane and the stage, where the substrates are placed, is the inclined angle ϕ. The angle between the substrates and the incidence Ar^+ beam, which is perpendicular to the horizontal plane, is the laid angle α. From the experiments shown later, the step etching rate and the step angle θ are closely correlated to the inclined angle and the laid angle.

The results for the step angle and the milling rate depend on the laid angle when the inclined angle is 45° as plotted in Fig. 3. The fitted line of the etching speed has similar shape with that of the step angle except it is several degrees lagging. The highest step angles appear where the milling rate reaches its maximum and the laid angle is about 45°. When the laid angle is larger than 45°, the step

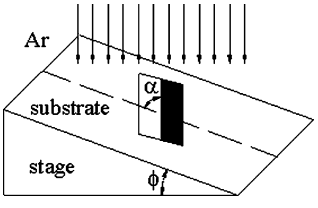

Fig. 2. Sketch of inclined angle ϕ and laid angle α when ion milling

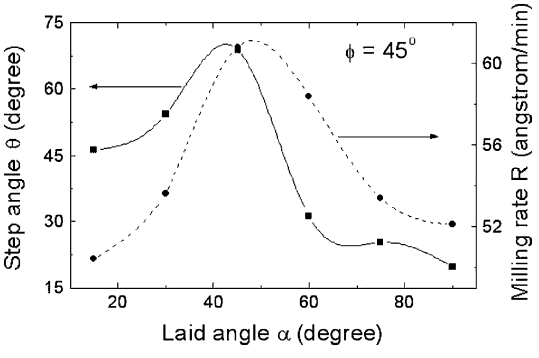

Fig. 3. Experimental points and fitted lines of step angle and milling rate dependent on laid angle when inclined angle is 45°

angle decreases rapidly. Laid angles would be better chosen larger than 30° and less than 45° so as to obtain a higher step angle and stay away from rapid decrease area.

Keeping the laid angle at 30°, the changes of the step angle and the milling rate dependent on the inclined angle as plotted in Fig. 4. Similar to the above result, the high etching rate causes a high step angle. Both of them reach their maximum at an inclined angle of about 50°.

In order to explore fully the step angle speak over the ϕ–α plane, several points of step angle and milling rate are also measured when α equals 90°. The relation between the milling rate and the step angle is the same and no higher peak for the step angle is found. From the plotting step angle as a function of the inclined and laid angle, as shown in Fig. 5, it is clear that the optimum milling conditions for high step angle are $45° < \phi < 50°$ and $30° < \alpha < 45°$. This rule of ion milling is the key factor to fabricate high step angle substrates.

3.2
Influence of metal mask film profile on step angle

A high step angle is determined not only by the milling position but also by the profile of the Nb mask film. If the Nb film has a slight slope, the low angle of the mask will transfer to the substrate due to the milling of the mask film. The upper angle of the obtained step slope is relatively high, but the lower angle is relatively low. If the Nb mask is undercut, the upper edge of the obtained step will incur a section because of the recession of the mask. If the side face of the Nb mask film is steep and sharp, the obtained step angle will be high and smooth if etching at a proper inclined and laid angle. All the circumstances are shown in Fig. 6, case (a), (c) and (b) respectively.

Now, the most important thing is to strictly control the profile of the Nb film. Because CF_4 etching includes a chemical process, undercutting always exists if over etching occurs. The Nb film and obtained step angles are measured by atom force microscopy (AFM) at different etching times, which are shown in Table 1. As etching time increases, the Nb film sidewall angle and obtained step angle also increase. When etching time is 275 s, the obtained step angle goes to its maximum value. If etching time further increases, the step angle decreases while the Nb sidewall angle is constant, which indicates an undercut has happened. Because the undercut cannot be tested by the AFM tip, only 75° Nb sidewall angles are measured. In order to enhance the substrate step angle, strict time control of reactive etching is necessary.

3.3
Fabrication results

Under strict reactive etching time control and optimum milling conditions, the high quality step substrates are fabricated successfully. As shown in Fig. 7, the upper and

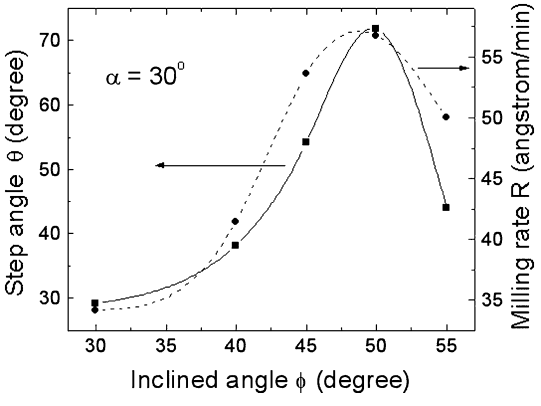

Fig. 4. Experimental points and fitted lines of step angle and milling rate dependent on inclined angle when laid angle is 30°

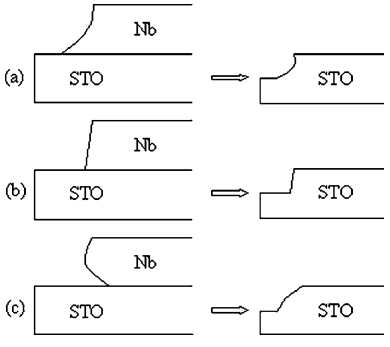

Fig. 6a–c. Illustration of influence of metal mask profile on step angle. **a** low mask angle causes low step angle, **b** sharp and steep angle causes sharp and steep step profile and **c** undercut of mask film causes small section on step profile

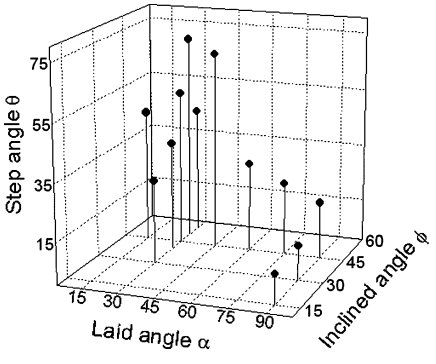

Fig. 5. 3-D plot of step angle dependent on inclined and laid angle. Optimum condition can be located as: $45° < \phi < 50°$ and $30° < \alpha < 45°$

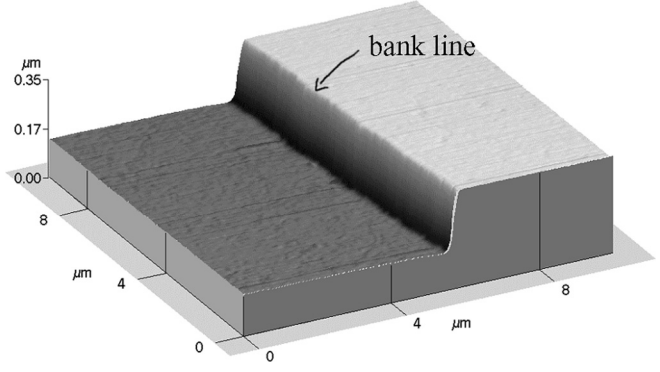

Fig. 7. AFM profile of high reproducible micromachining step substrate

Table 1. Influence of metal mask film profile on step angle when changing reactive etching time

Samples	CF_4 etching time (s)	Nb film angle (°)	Step angle (°)
01	250	65	30.8
02	260	67	50.7
03	270	66	61.7
04	275	68	63.7
05	280	75	48.1
06	290	75	41.5

Table 2. Parameters of fabricated dc-SQUIDs on highly reproducible micromachining step substrates

Parameters	Results	
Junction resistance $R_n(\Omega)$	Average	4.12
	Variation (±%)	28.6
Critical current $2I_c$ (μA)	Average	39.6
	Variation (±%)	42.4
Yield	75.0%	

lower angles of the step are sharp and smooth. The step angle is about 71° and there is no needle, pit, waviness, or other flaws at the surface. Within a 10 μm scope, the step is consistent, which ensures the possibility of single step grain boundary because the prepared junction width is 3 μm. The bank line of step is straight, which ensures the identity of two boundaries with a distance of about 10 μm.

At optimum conditions and a strict control process, twelve step substrates are prepared and YBCO films dc-SQUIDs are fabricated. Triangular waves of SQUIDs are measured, which works as the criteria for device producibility. The variation of critical current and junction resistance are also measured and all the parameters are listed in Table 2. The low variation of high reproducible step substrates dc-SQUIDs is realized. Till now, the best parameter control of chip-to-chip high T_C dc-SQUIDs is the variation of one magnitude and the yield for step edge junction SQUIDs is 1/3 to ½ [23] our parameter control, ±28.6% on junction resistance and ±42.4% on critical current is smaller than the reported value and the product yield is 75% larger than the best record. The strict controls of the mask profile and the optimum milling conditions have made the micromachining of step substrate fabrication a highly reproducible process.

4 Conclusions

The two identical junctions in dc-SQUIDs require that the step must have a straight bank line and a sharp and steep profile. The relations of milling speed, step angle, and substrate orientation parameters are investigated in detail. The high step angles are obtained where there exists high milling rates. The optimized milling conditions for ion milling are $45° < \phi < 50°$ and $30° < \alpha < 45°$. The influence of metal mask film profiles on a step angle is also investigated, and the best reactive etching time is found corresponding to a 4000 Å Nb film. The fabricated step substrates have a sharp and steep step angle and flawless profile. The variation of chip-to-chip junction resistance and critical current for obtained dc-SQUIDs is ±28.6% and ±42.4% respectively. The yield of the step edge junction dc-SQUIDs is 75.0%.

References

1. **Novak JL** (1989) IEEE International Conference on Robotics and Automation, pp. 137–144
2. **Auston DH** (1983) IEEE J Quantum Electronics 19: 639–648
3. **Bakker AH; Huijsing JH** (1996) Proc 1995 21st European Solid-State Circuits Conference. IEEE J Solid-State Circuits 31: 933–937
4. **Lauks IR** (1979) IEEE Transactions on Electron Devices 26: 1952–1959
5. **Moriizumi T** (1995) Proceedings of Transducers '95, the 8th International Conference on Solid-State Sensors and Actuators 1: 39–42
6. **Gravesen P; Branebjerg J; Sondergard Jensen OS** (1993) J Micromech Microeng 3: 168–182
7. **Ahn CH; Allen MG** (1993) J Micromech Microeng 3: 37–44
8. **Clarke J** (1986) IEEE Transactions on Electron Devices 27: 1896–1908
9. **Bednorz JG; Muller KA** (1986) Phys B 64: 189–193
10. **Nisedoff M** (1988) Cryogenics 28: 47
11. **Braginski AI** (1995) Draft02. Status pp 2
12. **Dimos D; Chaudhari P; Mannhart J; LeGoues FK** (1988) Phys Rev Lett 61: 219–222
13. **Char K; Colclough MS; Garrison SM; Newman N; Zaharchuk G** (1991) Appl Phys Lett 59: 733–735
14. **Daly KP; Dozier WD; Burch JF; Coons SB; Hu R; Platt CE; Simon RW** (1991) Appl Phys Lett 58: 543–545
15. **Simon RW** et al. (1990) Sci Tech of Thin Film Supercond 2: 549
16. **Di Iorio MS; Yoshizumi S; Yang K-Y; Zhang J; Maung M** (1991) Appl Phys Lett 58: 2552–2554
17. **Jia CL; Kabius B; Urban Herrmann K** (1991) Physica C 175: 545
18. **Herrmann K; Zhang Y; Muck H-M; Schubert J; Zander W; Braginski AI** (1991) Supercond Sci Tech 4: 583–586
19. **Herrmann K; Kunkel G; Siegel M; Schubert J; Zander W; Braginski AI; Jia CL; Kabius B; Urban K** (1995) J Appl Phys 78: 1131–1139
20. **Koelle D; Kleiner R; Ludwig F; Dantsker E; Clarke J** (1999) Rev Mod Phys 71: 632–678
21. **Jia CL** et al. (1992) Physica C 196: 211
22. **Sun JZ; Gallagher WJ; Callegari AC; Foglietti V; Koch RH** (1993) Appl Phys Lett 63: 1561–1563
23. **Braginski AI** (1996) In: Weinstock H (ed) SQUID Sensors: Fundamentals, Fabrication and Applications, NATO ASI Series, Kluwer Academic, Dordrecht, pp 235